AD-A230 101

REPORT DOCUMENTATION PAGE

REPORT SECURITY CLASSIFICATION Inclassified	1b RESTRICTIVE MARKINGS
SECURITY CLASSIFICATION AUTHORITY	3. DISTRIBUTION/AVAILABILITY OF REPORT
DECLASSIFICATION/DOWNGRADING SCHEDULE	Unclassified/Unlimited
PERFORMING ORGANIZATION REPORT NUMBER(S) ONR Technical Report #14	5. MONITORING ORGANIZATION REPORT NUMBER(S)
NAME OF PERFORMING ORGANIZATION Dept of Chemical Engineering and Mat rials Science	6a. OFFICE SYMBOL (If applicable) Code 1113
7a. NAME OF MONITORING ORGANIZATION Office of Naval Research	
ADDRESS (City, State, and ZIP Code) University of Minnesota Minneapolis, MN 55455	7b. ADDRESS (City, State, and ZIP Code) 800 North Quincy Street Arlington, VA 22217
NAME OF FUNDING/SPONSORING ORGANIZATION Office of Naval Research	8b. OFFICE SYMBOL (If applicable)
9. PROCUREMENT INSTRUMENT IDENTIFICATION NUMBER Contract No. N00014-87-K-0494	
ADDRESS (City, State, and ZIP Code) 800 North Quincy Street Arlington, VA 22217-5000	10 SOURCE OF FUNDING NUMBERS PROGRAM ELEMENT NO. / PROJECT NO. / TASK NO. / WORK UNIT ACCESSION NO

DTIC ELECTE DEC 14 1990 S E D

TITLE (Include Security Classification)

Correlation of Electron-Transfer Rates with the Surface Density of States of Native and Anodically Grown Oxide Films on Titanium

PERSONAL AUTHOR(S)

Norberto Casillas, Shelly R. Snyder, William H. Smyrl, and Henry S. White

TYPE OF REPORT	13b. TIME COVERED	14. DATE OF REPORT (Year, Month, Day)	15. PAGE COUNT
Technical	FROM 1/1/90 TO 10/31/90	11/16/90	

SUPPLEMENTARY NOTATION

submitted to **J. of Phys. Chem**, November 1990

COSATI CODES			18. SUBJECT TERMS (Continue on reverse if necessary and identify by block number)
FIELD	GROUP	SUB-GROUP	

ABSTRACT (Continue on reverse if necessary and identify by block number)

We report tunneling spectroscopy (TS) and surface density of states (SDOS) plots ((dI/dV)/(IV) vs V) for native and anodically grown titanium dioxide (TiO_2) films on polycrystalline Ti. The results are compared to data obtained using single crystal TiO_2 ((001 and (110) surface orientations). SDOS plots for anodically grown TiO_2 films (160Å thick) and single crystal TiO_2 show a large band-gap region (~2 eV) with a low state density separating the conduction and valence band edges. The similarity in the distribution of SDOS for anodically grown film has a well-ordered rutile structure. In contrast, SDOS plots obtained on native TiO_2 films show a nearly constant density of states over a 5 eV range and a ~25-fold increase in state density at energies corresponding to the band-gap region of anodically grown films and single crystal TiO_2. Electron-transfer rates for the oxidation of ferrocene in acetonitrile at native and anodically grown TiO_2 films are reported and correlated with the measured SDOS of these materials.

DISTRIBUTION/AVAILABILITY OF ABSTRACT	21. ABSTRACT SECURITY CLASSIFICATION
☒ UNCLASSIFIED/UNLIMITED ☐ SAME AS RPT ☐ DTIC USERS	Unclassified
22a. NAME OF RESPONSIBLE INDIVIDUAL Henry S. White	22b. TELEPHONE (Include Area Code) (612) 625-6945
	22c. OFFICE SYMBOL

DD FORM 1473, 84 MAR 83 APR edition may be used until exhausted. All other editions are obsolete

SECURITY CLASSIFICATION OF THIS PAGE

CORRELATION OF ELECTRON-TRANSFER RATES WITH THE SURFACE DENSITY OF STATES OF NATIVE AND ANODICALLY GROWN OXIDE FILMS ON TITANIUM

Norberto Casillas, Shelly R. Snyder, William H. Smyrl and Henry S. White
Department of Chemical Engineering and Materials Science
University of Minnesota
Minneapolis, Minnesota 55455

ABSTRACT. We report tunneling spectroscopy (TS) and surface density of states (SDOS) plots ((dI/dV)/(I/V) vs V) for native and anodically grown titanium dioxide (TiO_2) films on polycrystalline Ti. The results are compared to data obtained using single crystal TiO_2 ((001) and (110) surface orientations). SDOS plots for anodically grown TiO_2 films (160Å thick) and single crystal TiO_2 show a large band-gap region (~2 eV) with a low state density separating the conduction and valence band edges. The similarity in the distribution of SDOS for anodically grown TiO_2 films and single crystal TiO_2 indicates that the anodically grown film has a well-ordered rutile stucture. In contrast, SDOS plots obtained on native TiO_2 films show a nearly constant density of states over a 5 eV range and a ~25-50 fold increase in state density at energies corresponding to the band-gap region of anodically grown films and single crystal TiO_2. Electron-transfer rates for the oxidation of ferrocene in acetonitrile at native and anodically grown TiO_2 films are reported and correlated with the measured SDOS of these materials.

Submitted to *J. Phys. Chem.*, November, 1990.

Accession For
NTIS GRA&I
DTIC TAB
Unannounced
Justification
By
Distribution/
Availability Codes
Dist | Avail and/or Special
A-1

INTRODUCTION. The chemical stability of titanium is due to a native oxide film that spontaneously forms on the surface of the metal in air and in most oxygen-containing environments, eq. (1).

$$Ti + O_2 \rightarrow TiO_2 \quad (1)$$

The equilibrium of reaction (1) lies far to the right (ΔG = -212.6 kcal/mol)[1], and the resulting oxide film (~20 Å[2]) reduces the rate of metal oxidation to a negligible value in ambient environments. Localized breakdown of the native film occurs in chemically aggresive environments (e.g., aqueous Br- solutions) resulting in rapid local dissolution of the metal substrate. Although the mechanisms for oxide breakdown and resulting local metal dissolution are poorly understood for Ti and most other metals (e.g., Fe, Cu), it is frequently assumed that electric-field-assisted electron and/or ion-transfer reactions on the oxide film are involved. The chemical and electronic properties of the native film that control interfacial charge-transfer are, thus, of both fundamental and technological interest.

The properties of both native and thicker, anodically grown TiO_2 films have been studied using photoelectrochemical microscopy (PEM).[3,4,5] In the PEM experiment, the photocurrent response of a TiO_2 film is measured in an electrolyte solution as a laser is rastered across the surface. The results of such experiments have been correlated with differences in film crystallinity and oxide orientation as measured by x-ray and electron diffraction. While photoelectrochemical microscopy provides information concerning the electronic and structural properties of the oxide layer with a lateral resolution of several microns, the development of more direct methods of probing the surface electronic properties with higher lateral resolution is required to develop atomic-level mechanisms of charge-transfer reactions on oxide films.

Prior to this report, a number of authors have used scanning tunneling microscopy[6] (STM), and tunneling spectroscopy (TS)[7] to characterize the topography and electronic properties of TiO_2 surfaces in air and aqueous environments.[8]-[14] Recently, Fan and Bard have reported atomically-resolved STM images of doped, single crystal TiO_2 (001) in air.[12] In addition, these authors reported TS data from which they obtained a semiconductor band gap of ~3.0 eV, in agreement with the bulk value for rutile TiO_2. Gilbert and Kennedy have also reported TS data taken in air on doped single crystal TiO_2 (001).[13] Sakamaki et al. studied surfaces of the highly doped and hydroxylated TiO_2 (110) surface. Their findings suggest a reduction in the band gap of TiO_2 relative to the accepted bulk value, a difference attributed to the existence of chemisorbed OH^- groups.[14]

In this paper, we report a detailed comparison of TS results obtained on native TiO_2 films, anodically grown TiO_2 films, and the (001) and (110) surface orientations of single crystal rutile TiO_2 previously reported by the abovementioned researchers. We observe that the native oxide of Ti has a significantly higher density of electronic states at energies corresponding to the band-gap regions of single crystal rutile and anodically grown TiO_2 films. In the last section of this report, we describe electron-transfer rate measurements for the oxidation of a reversible redox species (ferrocene) on native and anodically grown films. We show that the observed differences in the electrochemical activity on the native and anodically grown oxide films can be correlated with the surface density of electronic states of these materials.

EXPERIMENTAL. Native and anodic oxide films were prepared on polycrystalline Ti. The average grain size of the Ti substrate was 250 nm^2. Polycrystalline samples were cut from a 3 mm thick Ti plate (99.9 % pure). Samples were mechanically polished with polishing paper to a grain size of 0.3 μm. A final polish was made with 0.05 μm alumina

suspended in water. Residue from the polish was removed by rinsing the samples in deionized water (Water Prodigy Labconco Co.) followed by ultrasonic cleaning and drying in air. Anodically grown TiO_2 films were grown by the procedure described previously.[3] Briefly, the potential applied to a Ti electrode in 0.1 M H_2SO_4 was scanned from 0.0 to 5.0 V vs a saturated calomel reference electrode (SCE) at a rate of 0.1 mV/s. The thickness of oxide film is determined by the final potential value. Oxide thicknesses were estimated from a calibration plot of thickness (determined by Auger depth profiling) vs final growth potential .[15]

Single crystal TiO_2 (001) (Commercial Crystal Laboratories, Inc.) was prepared by the procedure similar to that described by Fan and Bard.[12] The crystal was polished, etched in molten $KHSO_4$ at 620 °C and boiled in a mixture of $H_2SO_4/HNO_3/HF$ to remove the etch debris. The crystal was doped (~$1x10^{-19}$ cm^{-3}) by heating at 800 °C in a hydrogen atmosphere until its color became grey-blue (~30 min). Single crystal TiO_2 (110) (Commercial Crystal Laboratories Co.) was mechanically polished with a final polish using 0.05 μm alumina, washed with distilled water, and dried in air. The crystal was etched in H_2SO_4 at 200 °C for 2 h, rinsed in distilled water, dried in air, and reduced in hydrogen for 1 h at 600 °C.

TS data were obtained in air using the Nanoscope II (Digital Instrument Co.). Tunneling tips were mechanically cut from 0.01" diameter 70% Pt-30% Rh wire (Omega Co.). Ohmic contact was made to the sample using colloidal graphite. All TS data reported here were acquired at constant tip-to-separation using a bias voltage, V_b, of 1.5 V (tip vs substrate) and a tunneling setpoint current of 0.5 nA. Plots of (dI/dV/(I/V)) vs V were numerically calculated from the I-V curves following transfer of the data to an IBM PC.

Electrochemical measurements were performed using a Princeton Applied Research (PAR) Model 173 potentiostat and a Model 175 waveform generator. A SCE reference electrode and platinum wire counter electrode were used throughout the studies. The TiO_2

electrodes were prepared as described above and shrouded in teflon to seal the edges from the electrolyte solution. Ferrocene (Strem Chem. Co) was used as received. Acetonitrile was dried over 4 Å molecular sieves. Tetra(n-butyl)ammonium perchlorate was recrystallized twice from acetyl acetate and stored in vacuum. Electrochemical measurements were made in an unstirred solution.

RESULTS AND DISCUSSION.

Tunneling Spectroscopy and Surface Density of States.

Fig. 1 shows representative I-V curves obtained for (a) single crystals of TiO_2 (001) and (b) TiO_2 (110), (c) a mechanically polished Ti rod on which a ~160 Å thick TiO_2 film was anodically grown and (d) a mechanical polished rod. Reproducible I-V curves for TiO_2 single crystals, Figs. 1(a) and 1(b), and the anodically grown oxide film, Fig. 1 (c), show highly rectifying behavior, in agreement with expectations for a large band gap semiconductor. The tunneling current at each of these materials increased monotonically (less than exponential) as the tip-to-sample distance was decreased below 25Å. Tunneling current at positive biases (tip vs. substrate) results from tunneling of electrons from the valence band of TiO_2 (comprised of O 2p levels) to the metal tip. Conversely, tunneling current at negative bias (tip vs. substrate) results from electron tunneling from the metal tip into the TiO_2 conduction band (comprised of Ti 3d levels). We observe a larger tunneling current with the tip biased positive of the substrate than at negative biases, in agreement with previous reports.[12][14]

I-V curves for the native oxide layer on mechanically polished Ti frequently showed a less rectifying behavior in comparison to anodically grown films or single crystal substrates. For instance, comparison of I-V curve for the mechanically polished sample, Fig. 1(d), with the I-V curves of either Figs 1(a), (b), or (c) shows that the tunneling current at large negative or positive bias increases less rapidly as a function of bias. I-V curves obtained at *different locations* on the same sample occasionally showed rectifying

behavior essentially identical to that obtained using anodically grown films. The differences observed in the I-V response on the same native oxide surface suggest that the native oxide may have a non-uniform thickness or that a significant spatial variation exists in the density of defects which act as tunneling sites. The key qualitative feature that we note here, however, is that a significant percentage of the surface of the mechanically polished Ti surface shows a less ideal semiconducting behavior than either anodically grown films or single crystal TiO_2.

To obtain more detailed information of the surface electronic properties, I-V data are presented in Figs. 2 and 3 as (dI/dV)/(I/V) vs V spectra, where I is the tunneling current obtained at constant tip-substrate separation. The quantity (dI/dV) is the differential conductance; (dI/dV)/(I/V) is the same quantity normalized to the total or integral conductance (I/V) and represents an estimate of the surface density of states (SDOS).[16] The latter method of plotting tunneling data is preferred since it has been experimentally and theoretically shown to yield spectra for highly-doped inorganic semiconductors, e.g., Si, that are essentially independent of the tip-substrate separation.[16][17] In Fig. 2, the (dI/dV)/(I/V) vs V spectrum taken from the I-V data presented in Fig. 1 (d) for a native oxide film on mechanically polished Ti sample is compared to that for the 160 Å thick anodically grown TiO_2 film. The (dI/dV)/(I/V) vs V plot for the anodically grown oxide film (Fig. 2) shows a large increase in the SDOS at bias voltages of ~ -0.50 V below the Fermi level (0 V bias [7]) and 1.3 V above it. Between these values the differential conductance is 1-2 orders of magnitude smaller indicating a relatively small number of surface electronic states within the band gap. In contrast, the (dI/dV)/(I/V) vs V curve for the native oxide on the mechanically polished sample, Fig. 2 (b), shows a relatively constant SDOS over a 5 eV range with no indication of an increase in state density at biases corresponding to the conduction or valence band egdes as is readily apparent in the SDOS plot for the anodically grown film. In addition, it is noteworthy that the SDOS for the native film is 10 - 25 times larger *at biases corresponding to the apparent band gap energies*

of the anodic film (-0.5 < V < 1.3), a feature that will be discussed later in analyzing experimental values of the heterogeneous electron-transfer rates measured using these materials as electrodes in electrochemical experiments. The SDOS plots indicate that the thicker, anodically grown oxide displays more ideal semiconducting behavior, in agreement with previous photoelectrochemical measurements which show larger photocurrents on the anodically grown films than on native oxides.[3] The reason(s) that a well defined band-gap is not observed for the native TiO_2 film can not be discerned from the SDOS data alone. We suggest that the more uniform SDOS observed in Fig. 2 for the native film may be a consequence of tunneling across the thin native oxide, if it is sufficiently thin[18] or a large defect density in the native TiO_2 film due to a large number of oxygen vacancies or interstitial Ti^{3+}.[19]

Using the SDOS plots to establish the position of the conduction and valence bands, we obtain a band gap energy, E_g, that ranges from 1.7 to 2.0 eV for different samples of anodically grown TiO_2 films. SDOS plots for TiO_2 single crystals (e.g., Fig. 3) yield values E_g ranging from 2.0 to 2.8 eV for TiO_2 (001) and from 1.70 to 2.5 eV for TiO_2 (110). The higher end of these reported ranges are good agreement with E_g values obtained by similar analyses in other laboratories for TiO_2 (001) ($E_g \sim 3$ eV [12]) and TiO_2 (110) ($E_g \sim 1.7$ eV[14]). All present values are significantly smaller than the literature value of 3.04 eV for the bulk band gap of rutile TiO_2[20] and smaller than that determined photelectrochemically[4].

In general, (dI/dV/(I/V)) vs V curves for anodically grown films are qualitatively and quantitatively similar to that observed for the single crystal rutile substrates (Figs. 2 (b) and 3), in agreement with earlier studies that have shown that the anodically grown film has a predominatly rutile structure that is well ordered[3],[4]. In regard to the relatively small band gap observed in the present studies for TiO_2 single crystals (~ 1.7 - 2.8 eV), relative to the bulk value (3.04 eV), a plausible explanation for this difference can be associated with an increase in the density of surface subband gap tunneling states resulting

from adsorbtion of water molecules on the oxide surface as was suggested by Samamaky et al.[14] in the analysis of their TS data. We have no direct evidence for the existence of such a water layer on our surfaces, although it is likely that hydration of the surface occurs in the ambient conditions in which this study was performed. In addition to this possibility, we have compared our SDOS results to a recent tight-binding extended Huckel calculation[21] of the density of states for disordered TiO_2 (110) surfaces. These calculations indicate that the removal of oxygen atoms produces a broad range of surface states that are centered at ~0.7 eV below the conduction band edge, and which reduce the apparent band gap (as measured by the onset of SDOS at positive and negative bias) to ~1.5 eV (see Fig. 3 in ref. [21]). Our experimental average value of E_g ~1.8 eV for anodically grown TiO_2 is in resonably good agreement with this theoretical value, suggesting some degree of surface disorder.

Correlation of Electron-Transfer Rates on Native and Anodically Grown TiO_2 Films with SDOS Measurements.

The SDOS plots obtained for anodically grown and native oxide films suggests a large difference in the effective electronic properties of these two materials. Such differences should be readily apparent in other types of experiments and in applications in which electron-transfer occurs at the oxide film interface. Electron tunneling across a metal/vacuum (or air)/metal junction is similar in many respects to electron-transfer processes at electrode/solution interfaces[22],[23],[24]. In the latter case, electron-transfer is a tunneling event where the tunnel junction can be approximately represented as metal/solution/molecular acceptor (or donor) structure. A typical molecular acceptor/donor pair in electrochemistry is the Fe^{+3}/Fe^{2+} redox system, where the two halves of the redox couple are related by $Fe^{3+} + e^- \rightarrow Fe^{2+}$. This crude analogy ignores the complex double layer stucture that exists at the metal/solution interface but provides a simple framework in which to compare electrochemical electron-transfer rates with tunneling

currents observed using a scanning tunneling microscope. In both the electrochemical and tunneling experiments, electron-transfer is isoenergetic, requiring a donor and acceptor state of the same energy to exist on opposite sides of the tunnel junction. In the electrochemical experiment, the presence of both halves of a redox couple dissolved in solution defines a distribution of donor/aceptor states[25],[26], centered around the standard electrochemical potential, V'^{o}. This distribution is approximated by a gaussian function

$$\rho(V) = A\exp\{-(\lambda \pm e(V' - V'^{o})^2/\lambda 4kT\} \qquad (2)$$

where λ is the reorganizational energy between the oxidized and reduced halves of the couple (typically between 0.5 and 0.7 eV), A is a constant proportional to the concentration of electroactive species within electron-transfer distance of the surface (~10Å), and V' and V'^{o} are voltages measured with respect to a standard electrochemical reference electrode. (Primed values of V will be used to distinguish electrochemical biases vs. a reference electrode (V') from voltages reported in the TS experiments (V).) The positive and negative signs in eq. (2) correspond to the density of electronic states of oxidized and reduced redox spieces. Scheme I shows a plot of $\rho(V)/A$ assuming a reorganizational energy, λ, equal to 0.5 eV. The density of electronic states of reduced or oxidized speices is seen from this diagram to be centered at $eV'^{o} \pm \lambda$ with a base-width of ~2λ.

In order for an electron-transfer to occur at a metal (or semiconductor) electrode, it is necessary that an electron donor or acceptor state of energy equal to $eV'^{o} \pm 2\lambda$ exist at the electrode surface. For example, electron-donor states at the electrode surface of energy, E, between ~eV'^{o} and ~$(eV'^{o} + 2\lambda)$ are necessary to cause the reduction of an oxidized spieces (e.g., Fe^{3+}). Conversely, states of energy between ~$(eV'^{o} - 2\lambda) < E < eV'^{o}$ are necessary for oxidation of a reduced species.

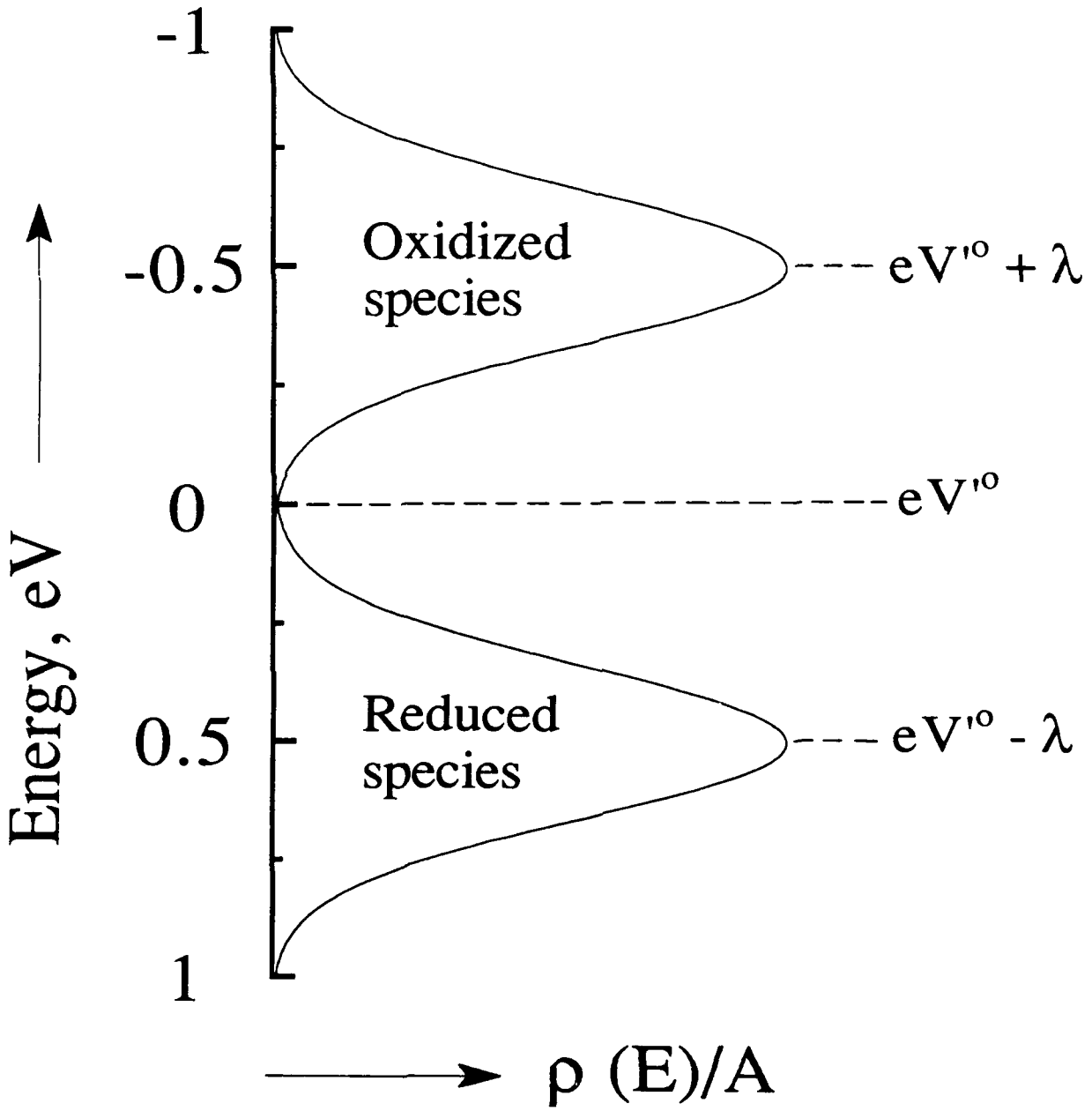

Scheme I. Density of states for a redox couple as a function of energy relative to the standard redox potential, V'°. $\lambda = 0.5$ eV was assumed in the calculation.

The tunneling current for either a vacuum[27],[28] or electrochemical[22],[23],[24] junction can be expressed as

$$I = \int_0^{eV} \rho_r(E)\rho_l(E,eV)T(E,eV)dE \qquad (3)$$

where $\rho_r(E)$ is density of states of the substrate (e.g., TiO_2) at energy E (relative to the Fermi level), $\rho_l(E, eV)$ is density of states at the tip (vacuum junction) or solution phase adjacent to the substrate (electrochemical junction), and T(E, eV) is the tunneling transmission probability. For the electrochemical junction, $\rho_l(E, eV)$ is equivalent to $\rho_l(V')$, eq. (2), after accounting for the difference in the absolute energy and electrochemical reference scales. Eq. (3) indicates that the rate of an electrochemical process can be limited by the magnitude of $\rho_r(E)$. At metal electrodes, e.g., Pt, this situation is not normally encountered since the density of states in the metal is much larger than that in the solution phase, i.e., $\rho_r(E) >> \rho_l(E, eV)$. However, at semiconducting electrodes, it is possible that the opposite condition, $\rho_r(E) < \rho_l(E, eV)$, is encountered at biases corresponding to the band-gap energies where the state density is low. Under this condition, the electron-transfer rate may be determined by the density of states in the electrode substrate. Qualitatively similar arguments have been presented by Frank and Bard[29a] to describe the photoelectrochemical behavior of TiO_2 single crystal electrodes in contact with electrolyte solutions.

The relatively large value of the SDOS observed on the native oxide at potentials corresponding to the band-gap region of anodically grown TiO_2 films ($-0.5 < V < 1.3$) suggests that former material may have a larger number of surface electronic states available to participate in electrochemical electron-transfer reactions *involving redox species whose V'^o values lie within the band-gap region of TiO_2*. To test this hypothesis, we have

measured and compared the voltammetric response of native and anodically grown TiO_2[29a,b] films in a non-aqueous solution containing a soluble electron donor.

Fig. 4 shows the response of the native and anodically grown TiO_2 films in acetonitrile containing 5 mM ferrocene (Fc) as an electron donor and 0.1 M tetra(n-butyl)ammonium perchlorate as an inert supporting electrolyte. Also shown is the voltammetric response of a Pt wire electrode of comparable area, at which the oxidation of Fc is kinetically facile and limited by diffusion of Fc to the electrode at conventional voltammetric sweep rates (~ 100 mV/s). Oxidation of Fc, eq. (4), represents the transfer of one electron per redox molecule to the electrode.

$$Fc \rightarrow Fc^+ + e^- \qquad (4)$$

The oxidation of Fc at the anodically grown oxide layer occurs at an immeasurably small rate, Fig. 4. In contrast, the voltammetric reponse at the Pt electrode displays peak currents of 10^{-4} A in both the forward and reverse potential sweeps, indicative of a diffusion-limited process[30]. The voltammetric reponse of the native TiO_2 film is intermediate between that observed on Pt and the anodically grown film. On the positive-going potential scan, there is a sharp rise in the current corresponding to the oxidation of Fc, eq. (4), at a potential corresponding roughly to the half-wave potential, $V'_{1/2}$, for the Fc/Fc^+ couple ($V'_{1/2} = (V'_{pa} + V'_{pc})/2$ where V'_{pa} and V'_{pc} represent the potential at the anodic and cathodic current peaks, respectively). The reverse sweep shows a small diffusion limited peak that corresponds to the re-reduction of the Fc^+ electrogenerated on the positve-going scan. This peak is absent in CH_3CN solutions that do not contain Fc. It is important to note here that the magnitude of anodic current density for the oxidation of Fc at the native TiO_2 film is much smaller than that observed on Pt and that no anodic peak current is observed, demonstrating that the current is not controlled by the diffusion of Fc

to the native TiO_2 film. This observation implies that the concentration of Fc (proportional to A in (eq. (2)) and the density of states in the solution layer immediately adjacent to the electrode surface, $\rho_l(E, eV)$, are of the same order of magnitude during voltammetric measurements using either native or anodically grown TiO_2 films. We also note here that because Fc is a neutral species, its concentration at the electrode surface, and therefore $\rho_l(E, eV)$, will not be affected by the existence of an electric field at the electrode/solution interface.

The voltammetric results shown in Fig. 4 indicate that the rate of electron-transfer between the dissolved redox species and the native oxide film is significantly larger than that on the anodically grown film. Using the above argument that the solution density of states, $\rho_l(E, eV)$, is the same in both measurements and assuming that T(E,eV) is approximately the same for both the native and anodically grown oxide films, we tentatively assign the observable difference in the electron-transfer rates to a difference in surface density of states, $\rho_r(E)$, of the two substrates, eq. (3).

The relative values of $\rho_r(E)$ for the native and anodically grown TiO_2 films at electrode potentials where Fc is oxidized ($E > E_{1/2}$) can be estimated from the SDOS plots shown in Fig. 2. To make this comparison it is necessary to relate the potential scale (V' vs SCE) in the electrochemical experiment to the bias voltage, V (vs the Fermi level), of tunneling spectroscopy measurements. The position of the conduction band edge of TiO_2 has been previously estimated from photoelectrochemical and capacitance measurements to be located a -0.5 V vs SCE in CH_3CN solutions[29a]. The standard potential, V'^o, of eq. (4) (approximated from $V'_{1/2}$ on Pt[30]) is ~0.4 V vs SCE. Thus, the Fc/Fc^+ redox couple represents a distribution of states in the solution centered at an energy ~0.9 eV below the conduction band edge of TiO_2, Scheme II. Assuming that the increase in SDOS at a bias of ~ -0.5 V for the anodically grown film represents the conduction band-edge (Fig. 2), the standard potential, V'^o, of the Fc/Fc^+ redox couple corresponds to a tip-to-substrate bias of ~ 0.5 V in the SDOS plot. Using eq. (2) and Scheme I, the solution

Anodic TiO_2 Film

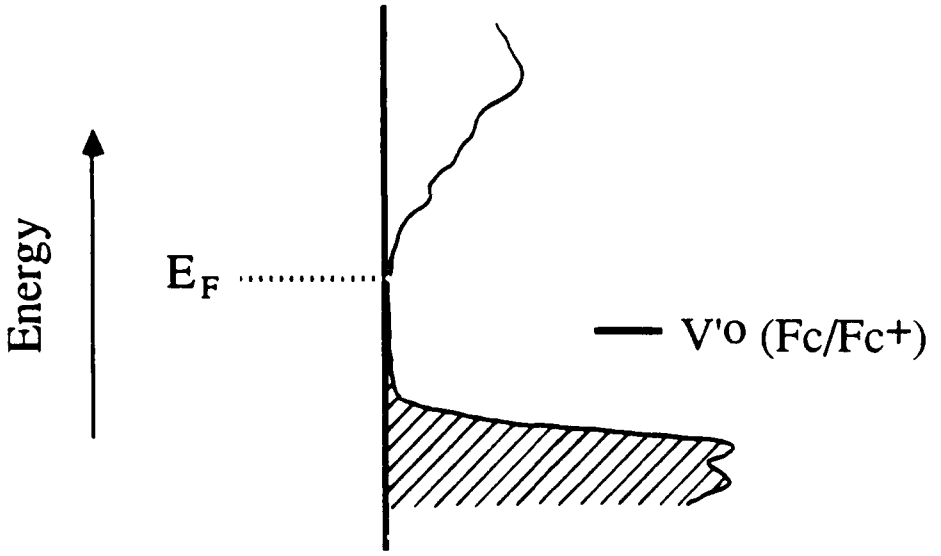

Native TiO_2 Film

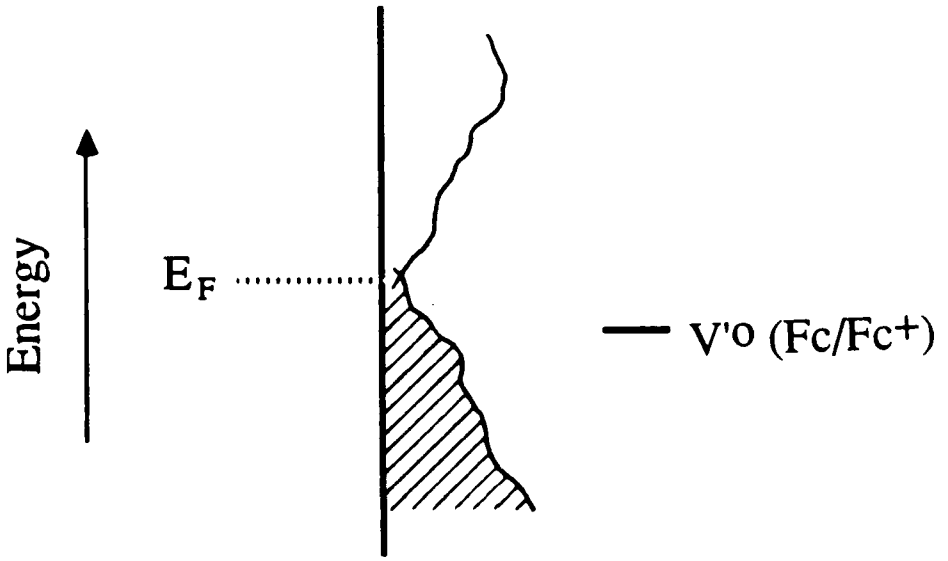

Scheme II. Qualitative representation of the density and energy of surface electronic states of anodically grown and native TiO_2 films. The standard potential, V'^o, of the Fc/Fc^+ redox couple is shown on the same energy scale.

donor states associated with the Fc molecule thus have energies that correspond to biases in the SDOS plots of ~ 0.5 - 1.0 V. Within this range, the magnitude of the SDOS for the native oxide film is ~20 - 50 times larger that the corresponding value for the anodically grown film. This difference qualitatively correlates with the larger electrochemical electron-transfer rates observed on the native oxide and supports our argument that the electron-transfer rate is determined by the substrate density of states, $\rho_r(E)$.

A final and natural step in this analysis would be to quantitatively compare the absolute magnitude of the electron transfer rate constants, k_s (cm/s), obtained by analysis of the voltammetric response[31], with the SDOS at the bias voltage corresponding to V'^o. The dependence of the characteristics of I-V curves as a function of the spatial position on native TiO_2 films (observed during the TS experiments (vide supra)) suggests that Fc may be oxidized at electochemically active surface sites of microscopic, and possibly atomic, dimensions. A quantitative measurement of k_s for native TiO_2 films is therefore not possible without an independent measurement of the geometric area or surface density of these sites. This goal is presently being pursued.

CONCLUSION. Several conclusions can be drawn from the results. First, the similarity in the SDOS of anodically grown TiO_2 films and single crystal rutile TiO_2 strongly suggests that the surface region of the film is crystalline with a rutile structure. The surface band-gap, E_g, of the anodically grown film is ~1.8 V, close to the value obtained on the (110) orientation of single crystal TiO_2. However, the experimental variablility in E_g values prohibits a definite assignment of the surface orientation of the anodically grown oxide. The structure of anodically grown TiO_2 films has been found to be rutile by grazing incidence electron diffraction[3],[4], with the (001) surface exposed. The expitaxial relationship between the oxide and substrate grains is not observed on all grains however, so that other orientations of the oxide are seen to a minor extent on polycrystalline Ti surfaces. The (1120) surface of a Ti single crystal also supports an

epitaxial film of TiO_2 with the (001) surface parallel to the substrate, as determined by grazing incidence-ray diffraction [31].

Second, the uniform distribution of SDOS for native oxide films on Ti suggest that these films do not have a long range crystlline structure. Limited data from grazing incidence electron diffraction of native TiO_2 films suggests that these latter films have a predominatly rutile struture, but with less evidence of order or epitaxial growth.[3],[4]

Finally, the large SDOS observed for native TiO_2 films at energies that correspond to the normal band-gap of TiO_2 provide a electronic pathway for electrochemical reactions. A correlation exists between the magnitude of the density of band-gap electronic states measured on native and anodically grown TiO_2 films with the rate of oxidation of ferrocene on these two substrates. These latter measurements are a preliminary step to quantitatively correlating measurable heterogeneous electron-transfer rate constants with the surface electronic properties of semiconducting and metal electrodes.

ACKNOWLEDGEMENT. The authors thank John Norton and Christopher McMillan for their assistance in preparing samples and performing electrochemical experiments. This work was supported by the Office of Naval Research Young Investigator Program, the Department of Energy-Office of Basic Sciences, and the Center for Interfacial Engineering with funding from NSF Engineering Research Centers Program (CDR 8721551).

REFERENCES.

1. Weast, R. C.; Astle, M. J. *"Handbook of Chemistry and Physics"*, 63rd Edition, CRC Press, Inc. Boca Raton, Fl, 1982.

2. Aladjem, A. *J.Mat. Sci.* **1973,** *8* , 688.

3. Kozlowski, M. R.; Tyler, P. S.; Smyrl, W. H.; Atanasoski, R. T. *Surf. Sci.* **1988**, *194* , 505.

4. Tyler, P. S.; Kozlowski, M. R.; Smyrl, W. H.; Atanasoski, R. T. *J. Electroanal. Chem.* **1987**, *237* , 295.

5. Leitner, K.; Schultze, J. W.; Stimming, U. *J. Electrochem. Soc.* **1986**, *133*, 1561.

6. Binnig, G.; Rohrer, H. *IBM J. Res. Develop.* **1986**, *30* , 355.

7. Stroncio, J. A.; Feenstra, R. M.; Newns, D. M.; Fein, A. P. *J. Vac. Sci. Technol.* **1988**, *A6,* 499.

8. Miranda, R.; Garcia, N.; Baro, A. M.; Garcia, R.; Peña, J. L.; Rohrer, H. *Appl. Phys.Lett.* **1985**, *47* , 367.

9. Morita, S.; Okada, T.; Ishigame, Y.; Sato, C.; Mikoshiba, N. *Jpn. J. Appl. Phys* **1986**, *25* , L516.

10. Gilbert, S.E.; Kennedy, J. H. *J. Electrochem. Soc.* 1988, 135, 2385.

11. Itaya, K.; Tomita, E. *Chem. Lett.* **1989**, 285.

12. Fan, F.-R. F.; Bard, A. J. *J. Phys. Chem.* **1990,** *94,* 3761.

13. Gilbert, S. E.; Kennedy, J. H. *Surface Sci. Lett.* **1990,** *225* , L1.

14. Sakamaki, K.; Itoh, K. ; Fujishima, A.; Gohshi, Y. *J. Vac. Sci. Technol.* A **1990**, *8(1)*, 614.

15. Kozlowski, M.; Smyrl, W. H.; Atanasoska, Lj.; Atanasoski, R. *Electrochim. Acta* **1989**, *34*, 1763.

16. Feenstra, I. S.; Stroscio, J. A.; Fein, A.P. *Surf. Sci.* **1987**, *181*, 295.

17. Moller, R.; Coenen, R.; Koslowski, B.; Rauscher, M. *Surf. Sci.* **1989**, *217*, 289.

18. Garcia, N. *IBM J. Res. Develop.* **1986**, *30*, 533.

19. Heinrich, V. E.; Kurtz, R. L. *Phys. Rev.* **1981**, *B23*, 6280.

20. Cronemeyer, D. C. *Phys. Rev.* **1952**, *87*, 876..

21. Wang, C.-R.; Xu, Y.-S., *Surf. Sci.*, **1989**, *219*, L537.

22. Gurney, R. W. *Proc. Roy. Soc. (London)* **1932,** *134A*, 137.

23. Sass, J. K; Gimzewski, J. K. J. Electroanal. Chem. **1988**, *251*, 241.

24. Bockris, J.O'M; Reddy, A. K. N. *Modern Electrochemistry*; Plenum: New York, 1970.

25. Morisaki, H.; Ono, H.; Yazawa, K. *J. Electrochem. Soc.* **1989**, *136*, 1710.

26. Gerischer, H. *Z. Phys. Chem. N. F.* **1961**, *27*, 48.

27. Simmons, J. G. *J. Appl. Phys.* **1963**, *34*, 2581.

28. Duke, C. B. *Tunneling in Solids,* Academic Press, New York, 1969.

29. Frank, S. N.; Bard, A. J. *J. Am. Chem. Soc.* **1975**, *97*, 7427.

30. (a) Bard, A.J.; Faulkner, L.F. *Electrochemical Methods*; Wiley: New York, 1980.
(b) Koffyberg, F.P.; Dwight, K.; Wold, A. *Solid State Comm.* **1979**, *30*, 433.

31. Toney, M. F.; Wiesler, D. S.; McMillian, C. S. Smyrl, W. H., April ,1990 APS Meeting.

FIGURES.

Figure 1. Current (I) vs voltage (V), for (a) native TiO_2 film (b) anodically grown TiO_2 on mechanically polished polycrystalline Ti (160 Å); (c) single crystal TiO_2 (100) (d) single crystal TiO_2 (110).

Figure 2. Surface density of states (dI/dV)/(I/V) vs voltage (V), for a native TiO_2 film and a 160 Å thick anodically grown TiO_2 film .

Figure 3. Surface density of states, (dI/dV)/(I/V) vs voltage (V), for (a) single crystal (001) and single crystal (110) TiO_2.

Figure 4. Cyclic voltammetric responses of platinum (0.25 cm^2), native TiO_2 film (0.63 cm^2), and anodically grown TiO_2 film (0.44 cm^2) in acetonitrile containing 5 mM ferrocene and 0.2 M tetra(n-butlyammonium perchlorate). Scan rate = 100 mV/s.

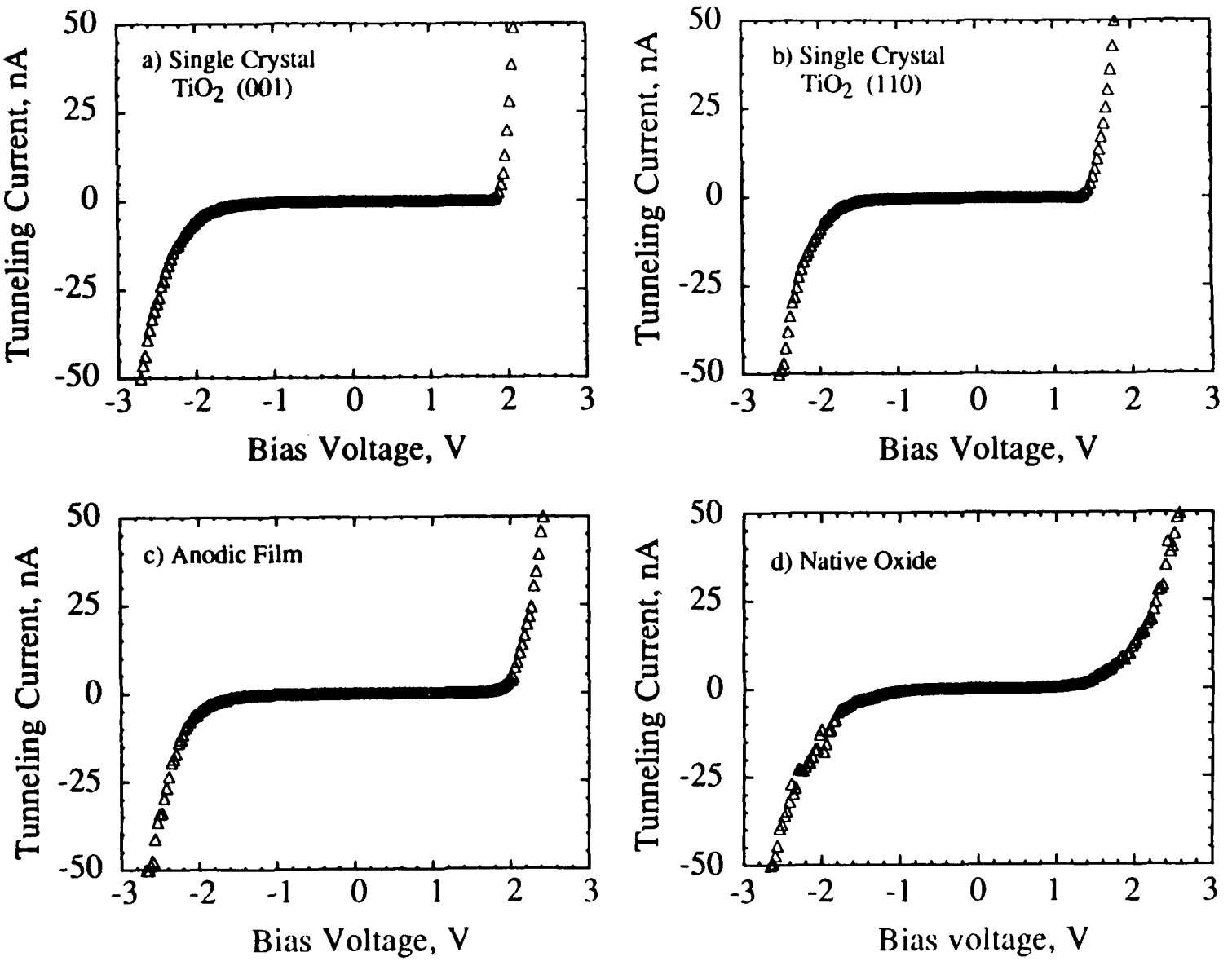
a) Single Crystal
TiO2 (001)
b) Single Crystal
TiO2 (110)
c) Anodic Film
d) Native Oxide
Tunneling Current, nA
Bias Voltage, V
Bias voltage, V
50
25
0
-25
-50
-3
-2
-1
0
1
2
3

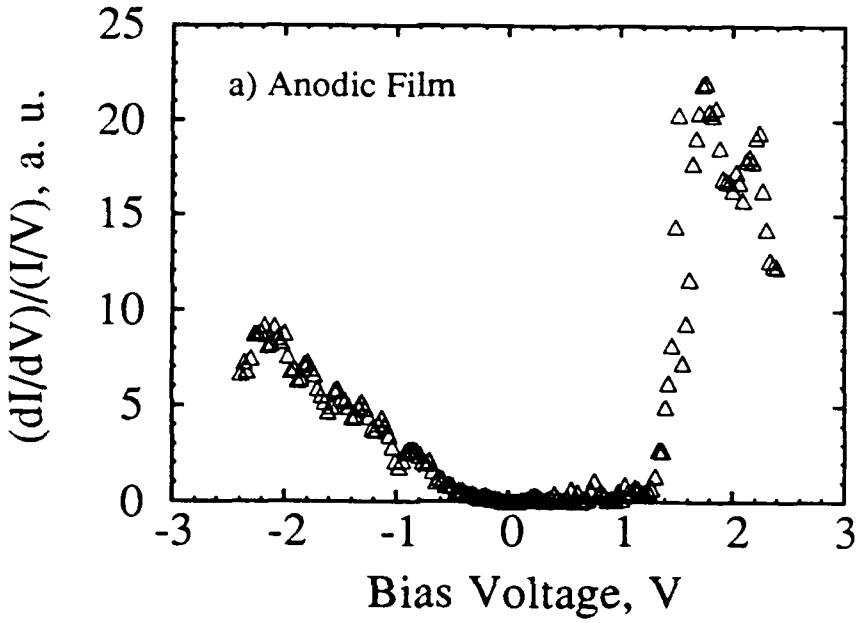
a) Anodic Film
(dI/dV)/(I/V), a. u.
Bias Voltage, V
25
20
15
10
5
0
-3
-2
-1
0
1
2
3

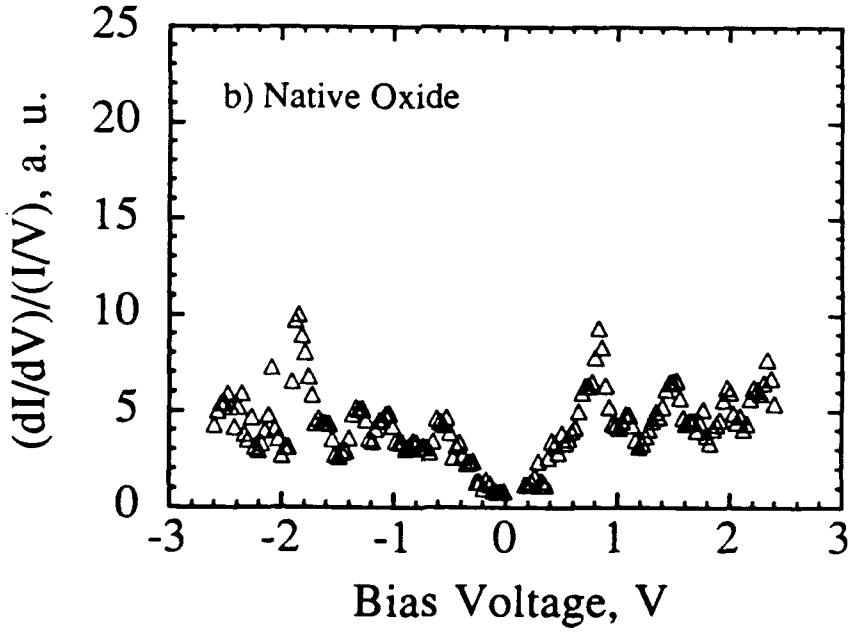
b) Native Oxide
(dI/dV)/(I/V), a. u.
Bias Voltage, V
25
20
15
10
5
0
-3
-2
-1
0
1
2
3

Fig 2

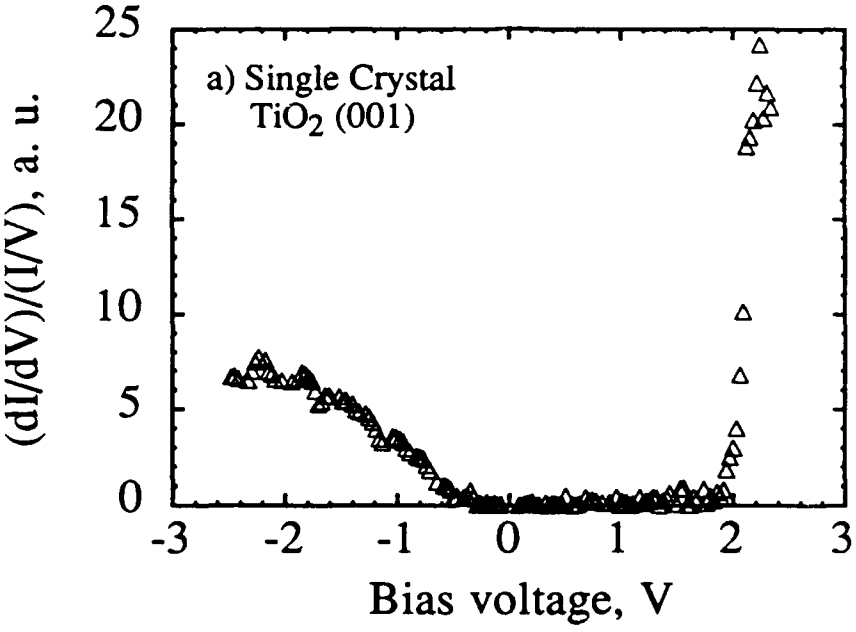
a) Single Crystal
TiO2 (001)
(dI/dV)/(I/V), a. u.
25
20
15
10
5
0
-3
-2
-1
0
1
2
3
Bias voltage, V

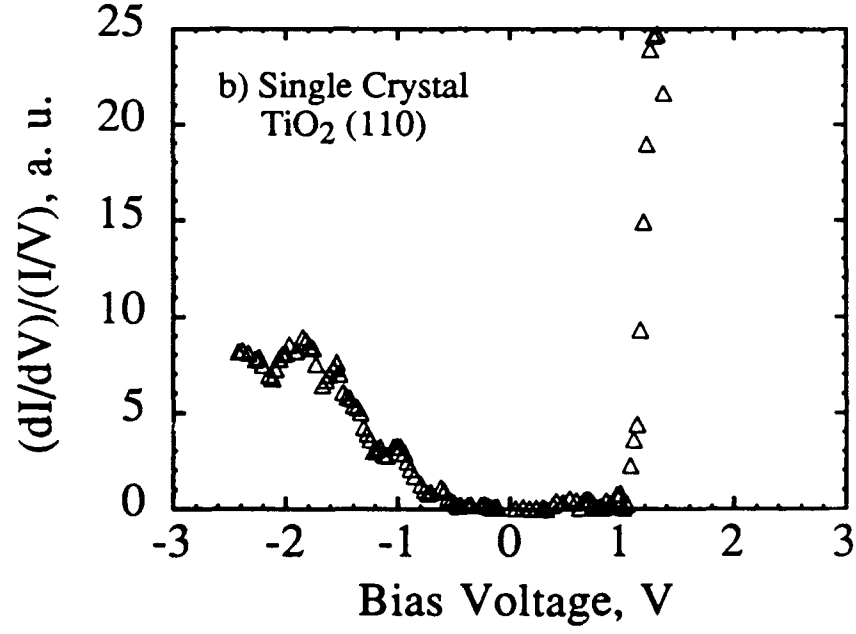
b) Single Crystal
TiO2 (110)
(dI/dV)/(I/V), a. u.
25
20
15
10
5
0
-3
-2
-1
0
1
2
3
Bias Voltage, V

Fig 3

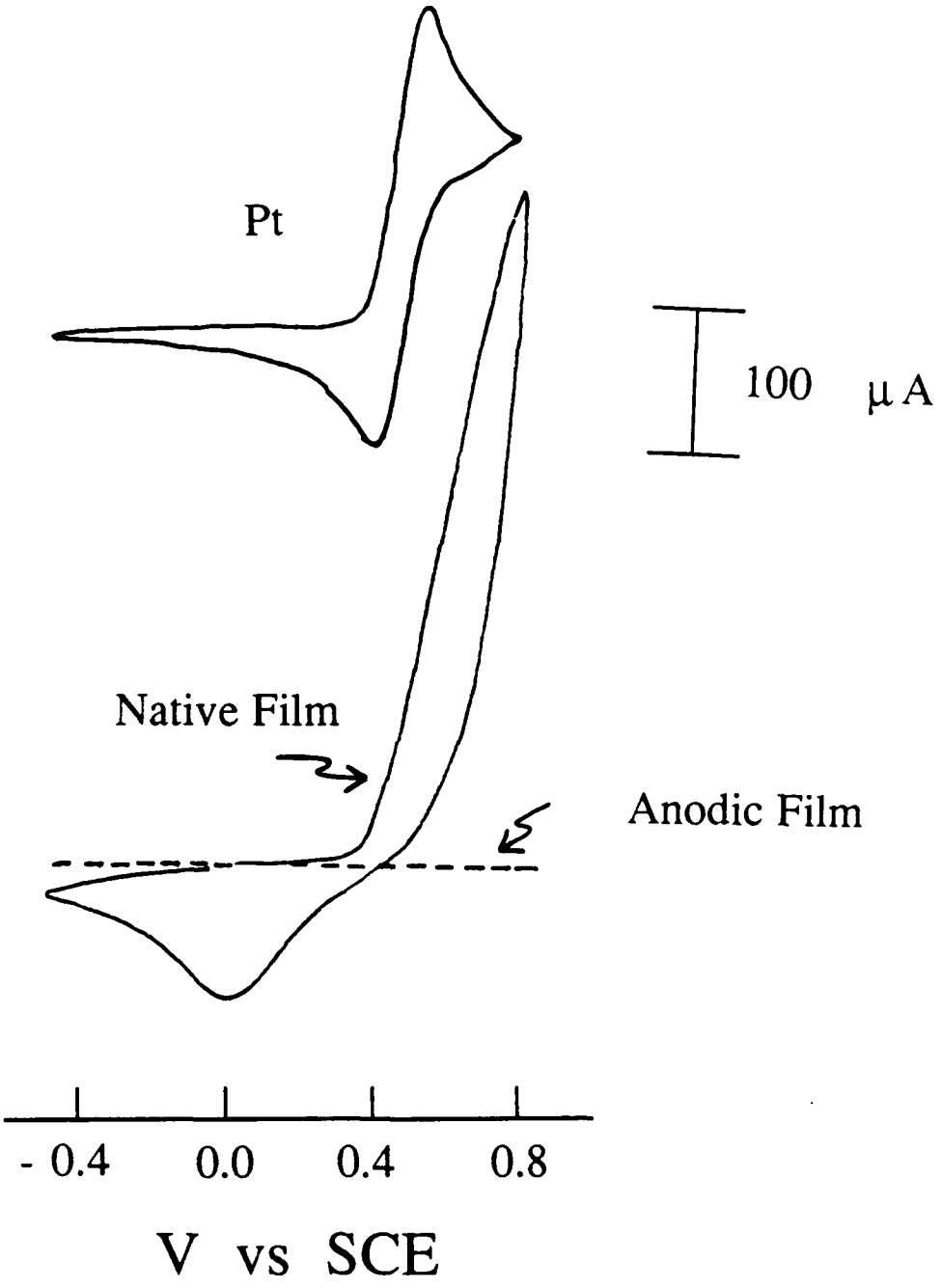

Fig 4